
Gaussian mixture models as a proxy for interacting language models

Edward L. Wang
Johns Hopkins University
ewang43@jhu.edu

Tianyu Wang
Johns Hopkins University
twang147@jhu.edu

Avanti Athreya
Johns Hopkins University
dathrey1@jhu.edu

Vince Lyzinski
University of Maryland, College Park
vlyzinsk@umd.edu

Carey E. Priebe
Johns Hopkins University
cep@jhu.edu

Abstract

Large language models (LLMs) are a powerful tool with the ability to match human capabilities and behavior in many settings. Retrieval-augmented generation (RAG) further allows LLMs to generate diverse output depending on the contents of their RAG database. This motivates their use in the social sciences to study human behavior between individuals when large-scale experiments are infeasible. However, LLMs depend on complex, computationally expensive algorithms. In this paper, we introduce interacting Gaussian mixture models (GMMs) as an alternative to similar frameworks using LLMs. We compare a simplified model of GMMs to select experimental simulations of LLMs whose updating and response depend on feedback from other LLMs. We find that interacting GMMs capture important features of the dynamics in interacting LLMs, and we investigate key similarities and differences between interacting LLMs and GMMs. We conclude by discussing the benefits of Gaussian mixture models, potential modifications, and future research directions.

1 Introduction

Research and development of large language models (LLMs) has progressed considerably in the past several years, with the result that large language models can now replicate several human characteristics and interactions observed in linguistic, cognitive and social sciences [1, 2]. Additionally, retrieval augmented generation (RAG) allows LLMs to retrieve relevant information from a database of information as additional context when completing a task, producing wider-ranging and more accurate responses [4]. Since the RAG database of information is akin to the knowledge and memories of a person, the incorporation of RAGs holds promise for computational frameworks that effectively model social interactions between individuals with diverse perspectives.

The construction of such computational frameworks for human interaction can be particularly useful when large-scale experiments on social phenomena are often impractical. In McGuinness et al., for example, [6] the time-varying output of interacting LLM agents is used to model two well-documented features of human social networks: first, human mirroring, in which individuals copy the behaviors of others, and second, social alignment, which is the emergence of a common perspective among individuals. In [6], the authors endow multiple LLMs—each representing a given agent—with RAG databases that are initialized with differing perspectives on a certain type of flower. Over a period of time, agents interact with each other, updating their RAG databases with responses from other agents. The collection of responses to the question of which flower “is prettiest” is measured at each time step.

Their approach yields conclusions matching those found in prior literature, along with new results on the effect of various parameters of social network evolution on social alignment. Of note are the formation of *stable silos*, in which an LLM’s communication with others does not much impact said agent’s own perspective, as well as *unstable silos*, which correspond to a dynamic equilibrium in which agents oscillate between different viewpoints. McGuinness et al further analyze the relationship of local and global communication patterns on the type and number of silos formed.

Despite the immense utility of modern language models in social science research, their inner workings are largely a black box. Thorough understanding is obscured by differing embedding functions [7], complexities of deep neural networks, varying architectures (including transformers [10], diffusion [5], and state space [12]), and massive quantities of data. This lack of standardization raises questions about the reliability of conclusions arising from complex systems of interacting LLMs. Furthermore, LLMs are computationally intensive, which translates to heavy energy, hardware, and time costs for training and text generation [3]. These concerns motivate us to consider whether we can develop alternative computational models that are simpler, interpretable, and computationally inexpensive, but also capture enough of the complexity of interacting LLM systems to be useful.

In this paper, we propose a computational framework utilizing multiple Gaussian mixture models (GMMs) as interacting agents, each with an associated set of vectors to act as a RAG database. Gaussian mixture models are well studied, and we can consider a training mechanism in which beliefs or perspectives are updated via the Expectation-Maximization (EM) algorithm. In this paper, we implement a system of interacting GMMs, running similar experiments as discussed in McGuinness et al., comparing the results obtained from their RAG LLM computational framework and our GMM framework. We find that interacting GMMs can replicate the complex time varying dynamics, such as stable and unstable siloing, of interacting LLMs, but with a more easily interpretable underlying algorithm and far less computational cost.

2 Methodology

2.1 Background: LLM simulations for interacting agents

We briefly describe the LLM simulation methodology from [6] with which we compare our simulation with. In experiments, McGuinness et. al investigate the time-varying beliefs of agents by asking about preferences among LLM agents over a collection of flowers; in particular, questions asks about each LLM agent’s “favorite” or “prettiest” flower.

The LLM simulation consists of n agents $\{A_i\}_{i=1}^n$ where the agents are LLaMA-2-7B-Chat models [9], each equipped with external RAG databases with a fixed number of sentences about flowers. Since these agents change over time, we denote the i th agent at time t as $A_i^{(t)}$.

Each LLM has its RAG database initialized with random sentences about flowers, generated by asking ChatGPT to “describe the beauty of various flowers.”

At each time $t = 0, 1, \dots, T$, the agent is asked to describe the prettiest flower. For each agent $i = 1, \dots, N$, $B_i^{(t)}$ represents the answer of agent A_i at time step t . First, the type of flower that the agent describes is extracted from the answer and converted to a natural number Flower ID. This is used to determine the silo that the agent is in at time t . Next, the response $B_i^{(t)}$ is embedded to a vector $X_i^{(t)}$ in \mathbf{R}^{768} using nomic-embed-v1.5 [8].

For each $t = 1, \dots, T$, the LLM performs an interaction. For each agent $A_i^{(t-1)}$, we pick another agent $A_j^{(t-1)}$ to interact with. With mirroring probability p , we let $j = i$, so that the agent interacts with itself. Otherwise, j is randomly chosen from the k nearest neighbor agents to $A_i^{(t-1)}$. The distance between two LLM agents is defined as the l_2 distance between the embeddings of their response.

$$d(A_i^{(t)}, A_j^{(t)}) = \left\| \mathbf{X}_i^{(t)} - \mathbf{X}_j^{(t)} \right\|_2 \tag{1}$$

Once j is selected, agent $A_i^{(t-1)}$ updates its RAG with the new sentence $B_j^{(t)}$. $A_i^{(t)}$ is the new agent with the updated RAG.

2.2 GMM simulation

2.2.1 Agent model

We define $\{A_i\}_{i=1}^n$ to be the n distinct agents in our system. Each agent A_i is represented as a pair of a GMM G_i and a ‘‘RAG’’ set R_i .

Each GMM G_i is parametrized by a mean vector, variance vector, and a weight vector. We model m different beliefs or perspectives of a given agent by a mean vector $\boldsymbol{\mu} = [\mu_1, \dots, \mu_m] \in \mathbb{R}^m$ and for simplicity, we consider this fixed for all GMMs $\{G_i\}_{i=1}^n$; this vector does not change with time. We let $\boldsymbol{\sigma}^2 = [\sigma_1^2, \dots, \sigma_m^2]$ be the fixed, common variance vector for all GMMs. Finally, we let $\mathbf{w}_i \in \Delta^{m-1}$ denote the weight vector for the i th GMM. Each component of the weight vector describes the probability of a draw from a Gaussian centered at one of the μ_j s and can be interpreted as the agent’s degree of certainty in perspective μ_j . These weight vectors vary between agents and change over time, defining the agent’s beliefs.

Each RAG set R_i is a set of elements in \mathbb{R} with a fixed size r , representing agent A_i ’s unique knowledge and memories.

Since we are interested in the behavior of agents as they act over time, we introduce a time parameter t . Each agent will only interact and update at discrete time steps for $t = 1$ to T . Let $A_i^{(t)}$ denote the i th agent at time t . Since the weight vectors and RAG sets can change over time, we let $\mathbf{w}_i^{(t)}$ denote the weight vector of $A_i^{(t)}$ and $R_i^{(t)}$ denote the RAG of $A_i^{(t)}$.

Our model, described in algorithm 1, is comprised of initialization, measurement, and interaction steps.

Algorithm 1 Standard simulation procedure

```

1: procedure SIMULATEINTERACTINGGMMS( $T, p, k, r$ )
2:   for  $i \in \{1, \dots, 30\}$  do                                     ▷ Initialize weights and RAGs
3:      $\mathbf{w}_i^{(0)} \leftarrow \mathbf{e}_i$ 
4:      $R_i^{(0)} \leftarrow \text{SAMPLEFROMGMM}(\mathbf{w}_i^{(0)}, r)$ 
5:   end for
6:   for  $t \in \{1, \dots, T\}$  do                                     ▷ Interact for each time step from 1 to  $T$ 
7:     for  $i \in \{1, \dots, 30\}$  do
8:        $u \leftarrow \text{UNIFORM}(0,1)$ 
9:       if  $u < p$  then
10:         $j \leftarrow i$ 
11:       else
12:         $K \leftarrow \text{GETKNEARESTGMMs}(k, i)$  ▷ Returns a set of the indices of the  $k$  closest
          GMMs where distance is computed by Euclidean distance of the weight vectors
13:         $j \leftarrow \text{UNIFORMCHOICE}(K)$                                ▷ Uniformly chooses a member of the set
14:       end if
15:        $\text{INTERACT}(i, j, t)$ 
16:     end for
17:   end for
18: end procedure

```

SampleFromGMM(\mathbf{w}, n) generates n samples from the GMM with mean $\boldsymbol{\mu} = [\mu_1, \dots, \mu_m]$, variances $\boldsymbol{\sigma}^2 = [\sigma_1^2, \dots, \sigma_m^2]$, and weights $\mathbf{w} = [w_1, \dots, w_m]$. UpdateGMM(d, \mathbf{w}) computes the new weights of the GMM given the prior weights \mathbf{w} and new data d when the means and variances are fixed.

2.2.2 Initialization

The initialization steps correspond to lines 2 to 4 in algorithm 1. For our experiments, we set $n = m = 30$ unless otherwise specified and initialize the weight vector for the i th agent to be $\mathbf{w}_i^{(0)} = \mathbf{e}_i$ where $\mathbf{e}_i \in \mathbb{R}^m$ is the i th standard basis vector. We then sample r points from the GMM

and set that as our starting RAG $R_i^{(0)}$ for the i th agent. This results in agents with diverse viewpoints and unique knowledge and memories to justify their perspective.

2.2.3 Measurement

At each time $t = 0, 1, \dots, T$, we evaluate each model to determine which of the m perspectives it is most aligned with. We call this the silo the agent belongs to. For computational convenience, we define it as the index of the weight vector that has the largest value, breaking ties by picking the smaller index.

$$\text{silo} \left(A_i^{(t)} \right) = \underset{j \in \{1, \dots, m\}}{\operatorname{argmax}} \left(\left(\mathbf{w}_i^{(t)} \right)_j \right) \quad (2)$$

Agents that belong to the same silo have similar beliefs and are considered aligned.

In our implementation, we save the weight vectors at each time step t and compute the measurement step for all agents $i = 1, \dots, n$ and time steps $t = 0, 1, \dots, T$ at the end.

2.2.4 Interaction

The interaction step is performed after each measurement step for each time step $t = 1, \dots, T$. Here, we allow each agent a chance to update its own RAG and perspectives given new information from the interaction.

At time t , each preupdated agent $A_i^{(t-1)}$ chooses an agent $A_j^{(t-1)}$ to interact with. With probability p , a fixed mirroring probability set at the beginning of the simulation, we let $j = i$, where the agent updates itself with the data it generates. Otherwise, with probability $1 - p$, $A_i^{(t-1)}$ selects uniformly at random from one of its k nearest neighbors and updates itself using the data that the chosen neighbor agent generates. We define the distance between two agents as the l_2 distance between their weight vectors.

$$d(A_i^{(t)}, A_j^{(t)}) = \left\| \mathbf{w}_i^{(t)} - \mathbf{w}_j^{(t)} \right\|_2 \quad (3)$$

After the agent $A_j^{(t-1)}$ is chosen, we perform the interaction, where $A_i^{(t-1)}$ learns from $A_j^{(t-1)}$. We start by sampling x from $G_i^{(t-1)}$. The j th agent considers this new piece of information by creating a new set Q from its RAG set $R_j^{(t-1)}$ by replacing the element in the RAG furthest away from x in Euclidean distance with x . The j th agent then temporarily incorporates this new body of knowledge into its own perspective. We run the M-step of the standard EM algorithm on GMM $G_j^{(t-1)}$ with the r pieces of data given in Q to produce temporary new weights $\mathbf{w}_j^{(t)}$. We then incorporate this information into the RAG of agent i by generating a sample y from the GMM with weights $\mathbf{w}_j^{(t)}$ and replacing the element in $R_i^{(t-1)}$ furthest from y with y . This new RAG set is then used to update agent i using the EM algorithm to get $\mathbf{w}_i^{(t)}$. The entire interaction step is given by lines 7 to 15 in algorithm 1 with the update function given by algorithm 2.

Algorithm 2 Update of GMM i when interacting with GMM j at time t

- 1: **function** UPDATE(i, j, t)
 - 2: $x \leftarrow \text{SAMPLEFROMGMM}(w_i^{(t-1)}, 1)$
 - 3: $\text{qrag_clsup_j} \leftarrow (R_j^{(t-1)} \cup \{x\}) \setminus (\operatorname{argmax}_{v \in R_j^{(t-1)}} \|x - v\|)$
 - 4: $\text{w_clsup_j} \leftarrow \text{UPDATEGMM}(\text{qrag_clsup_j}, w_j^{(t-1)})$
 - 5: $y \leftarrow \text{SAMPLEFROMGMM}(\text{w_clsup_j}, 1)$
 - 6: $R_i^{(t)} \leftarrow (R_i^{(t-1)} \cup \{y\}) \setminus (\operatorname{argmax}_{v \in R_i^{(t-1)}} \|y - v\|)$
 - 7: $w_i^{(t)} \leftarrow \text{UPDATEGMM}(R_i^{(t)}, w_i^{(t-1)})$
 - 8: **end function**
-

3 Results

3.1 Silo Patterns

In McGuinness et al., the authors describe the formation of three types of silos: stable silos, unstable silos, and decaying silos [6]. We focus on the cases of stable and unstable silos, defined by the following stability metric.

The stability at time t , $S^{(t)}$ is defined to be the proportion of agents that have changed silos from time step $t - 1$ to t .

$$S^{(t)} = \frac{1}{n} \sum_{i=1}^n 1_{\text{silos}(A_i^{(t)}) \neq \text{silos}(A_i^{(t-1)})} \quad (4)$$

We define stable and unstable silos below.

- A stable silo system occurs if there exists a fixed time t^* where the number of silos is constant for time steps $t > t^*$ and $S^{(t)} = 1$.
- An unstable silo system occurs if the number of silos is constant after a fixed time t^* but $S^{(t)} < 1$ for some $t > t^*$.

Running our GMM simulation with RAG size $r = 5$, mirroring probability $p = 0.4$, $k = 29$ nearest neighbors, and $T = 400$ results in the formation of an unstable silo, and we compare this with the results from McGuinness et al. in figure 1. The first column shows our results using GMMs and the second column shows the results from figure 2 in McGuinness et al. using LLMs.

The first row of figures show the evolution of each agent’s silo over time with each line representing a unique agent. In both setups, we see that after a certain time t^* , approximately 175 for the GMM case and 22 for the LLM case, only two silos exist for the rest of the simulation. Furthermore, we see lines jumping between the two silos, indicating that we have an unstable silo. However, we see that in our GMM case, it takes significantly more time for the unstable silo to form and that the switching between the two silos is much slower compared to the LLM case.

The second row of figures represents the evolution of the number of agents in each possible silo with each line representing a particular silo. In both cases, we see that the number of agents in all silos, except for two, go to zero, while the number of agents in the remaining silos oscillate. Once again, we see a longer time until formation of unstable silos and a slower speed of oscillation. One striking difference between the GMM and LLM case is that the in the GMM case, it seems that one of the silos is slowly dominating the other while the silos in the LLM case do not have substantial decay or growth. However, during $t = 175$ to about $t = 300$, the GMM case also does not exhibit substantial decay or growth. So, the eventual domination of one silo may be due to the longer time frame of simulation. We investigate this phenomenon of eventual convergence to a single silo as $t \rightarrow \infty$ further in section 3.3.

The last row shows plots of the stability vs. time for stable siloes and unstable siloes in the GMM and LLM case. In both situations, stable siloes result in completely stability after a certain time t^* . Similarly, unstable siloes, while remaining at two silos, always have periods of stability less than one. In our GMM case, these dips in stability are less frequent compared to in the LLM case.

3.2 Effect of global interaction parameters on silos

McGuinness et al. conduct an extensive study of the effect of the global interaction parameters k and p on siloing behavior, where k represents the number of closest neighbors an agent can talk to and p represents the mirroring probability or probability an agent interacts with itself. In one experiment, they investigate how varying k affects the number of silos formed. We focus on replicating these results for $p = 0$ while varying k . For each value of k , we run 50 replicates of the simulation with $p = 0$, $T = 80$, and $r = 5$. Figure 2 compares our results on the left to the results from McGuinness et al. on the right. Our simulations agree with the findings of an inverse relationship where increasing k and the ability to communicate globally results in the formation of less silos.

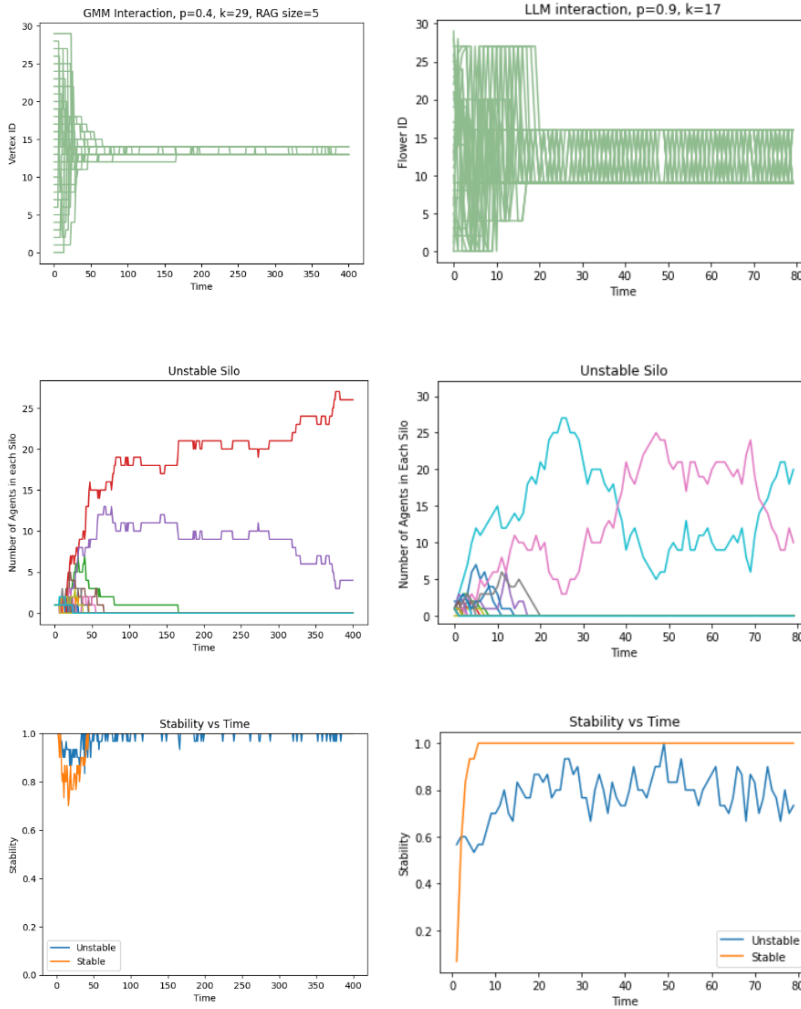


Figure 1: Comparison of unstable silo behavior for our GMM simulation and the LLM simulation from McGuinness et al. **Left.** Unstable silo behavior for the GMM model described in this paper. We set the global parameters to be $p = 0.4$, $k = 29$, $r = 5$, and $T = 400$. **Right.** Unstable silo behavior for the LLM model in McGuinness et al. **Top.** An example unstable silo system where each line represents an agent. **Middle.** The evolution of the number of agents in each possible silo where each line represents a silo. **Bottom.** Comparison of the stability metric for stable and unstable silos.

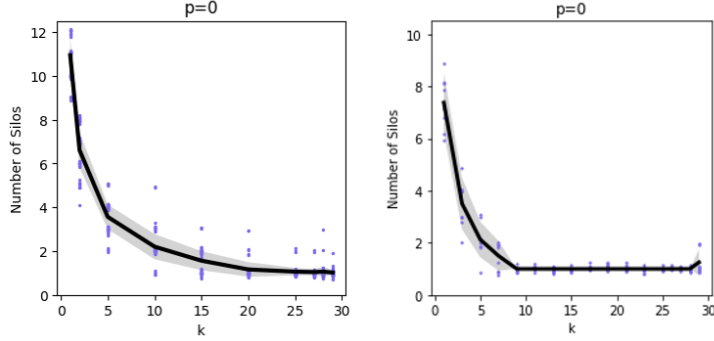


Figure 2: Comparison of the effect of k on the number of silos for $p = 0$ between the GMM and LLM simulations. **Left.** The result of the GMM simulation with $T = 80$, and $r = 5$. Each value of k was simulated 50 times with the line indicating the average and the shaded region indicating ± 5 SE. **Right.** The result of the LLM simulation from figure 4 of McGuinness et al.

Additionally, McGuinness et al. provide a qualitative analysis of how agent behavior changes over a sweep of values of both p and k . We demonstrate similar dynamics with GMM simulations in figure 3. Figure 3a shows the interacting system dynamics for the GMM case and figure 3b shows the LLM case. In both scenarios, we see that increasing p slows convergence to stable or unstable silos, resulting in a longer time to achieve global alignment. In particular, the last row of figure 3a when $p = 0.7$ shows behavior where the system has not converged to either a stable or an unstable silo yet. We call this a “decaying silo,” which is not a stable state but we expect that under more iterations that it will converge to either the stable or unstable silo case. Increasing k decreases the number of silos formed, demonstrating that opportunities to talk to increasingly diverse people promotes global alignment.

3.3 Formation of a single silo for large t

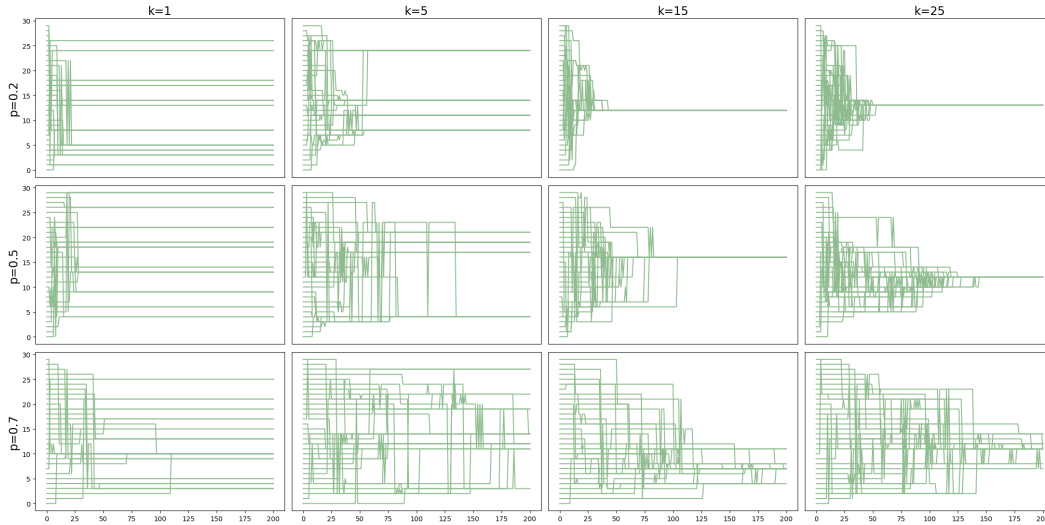
When comparing the two unstable silo examples for the GMM and LLM case, one major difference is the fact that in our GMM case, one of the silo eventually begins to dominate the other, while in McGuinness et al., there is no long-term pattern of growth or decay in the two silos. This is likely due to the larger number of time steps for which the GMM simulation was run. In fact, McGuinness et al. observe this long term behavior of convergence to a single silo in the LLM simulations as well. Thus, we conjecture that when the simulation is run for a large number of time steps, $t \rightarrow \infty$ and large enough k , the interactions will eventually collapse into a single stable silo. Figure 4 demonstrates an example of this behavior in both the LLM and GMM simulations, where unstable silo patterns are shown at earlier time steps, but eventually it collapses into a single stable silo.

To test this conjecture, we ran the simulation with $p = 0.1$, $k = 29$, $T = 200$, and $r = 10$ for 50 replicates. In every single experiment, we see a collapse into a single stable silo by $t = 200$, providing evidence supporting our conjecture.

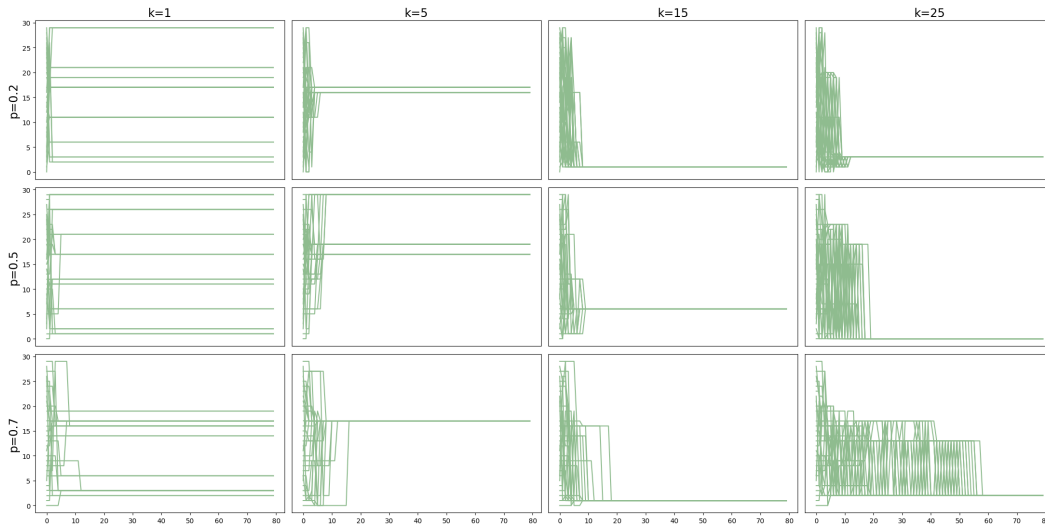
We also investigate the relationship that changing μ , the means of the Gaussians, had on the convergence to a single silo. Here, we let $\Delta\mu$ range from 1 to 6 with a step size of 0.5 and set $\mu_i = \Delta\mu \cdot i$, where increasing $\Delta\mu$ increased the distances between the means of the Gaussian. Fixing $k = 1$, $p = 0$, $r = 5$, we ran the simulation 50 times for each value of $\Delta\mu$. In each simulation, we recorded t^* , the smallest time where for all $t > t^*$, the number of silos at time t was 1. Figure 5 shows that the average time it took to converge to a single silo decreased as we increased the distance between means.

4 Discussion

In sections 3.1 and 3.2, we compare the results of systems of interacting GMMs with that of interacting LLMs on two different experiments. Section 3.1 focuses on the behavior of unstable silos, while section 3.2 investigates the effect of the global parameters p , the probability of mirroring, and k , the number of nearest neighbors that each agent can communicate with, on the number of silos formed.



(a) **GMM System.** Each plot has the time from $t = 0$ to 200 on the x-axis and the silo of the agent on the y-axis.



(b) **LLM System.** Each plot has the time from $t = 0$ to 80 on the x-axis and the silo of the agent on the y-axis.

Figure 3: Example systems of $n = 30$ interacting agents for varying values of p and k in both the GMM and LLM case. The value of p is constant for each row and the value of k is constant for each column. We see in both cases that increasing p decreases the rate of agent silo changes and slows the development of global alignment. Small values of k prevent global alignment and formations of single silos.

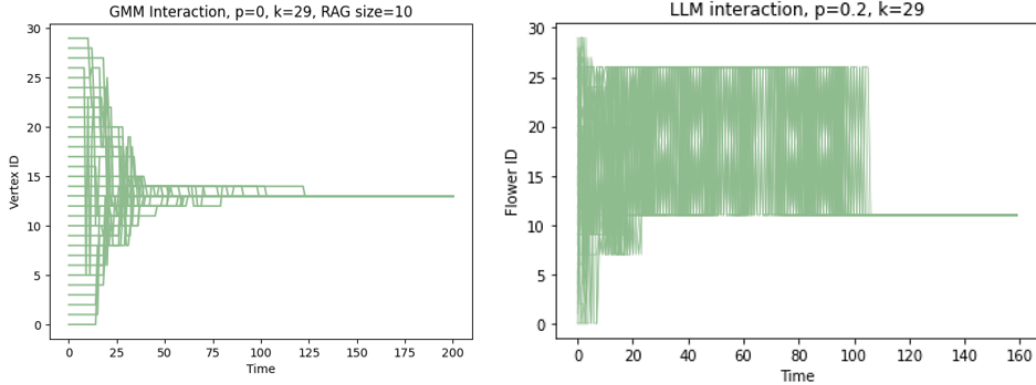


Figure 4: Example plot of the convergences to one silo for large t . Each line represents an agent. **Left.** The result of the the GMM simulation with $p = 0$, $k = 29$, $T = 200$, and $r = 10$. **Right.** The result of the LLM simulation with $p = 0.2$, $k = 29$, $T = 160$.

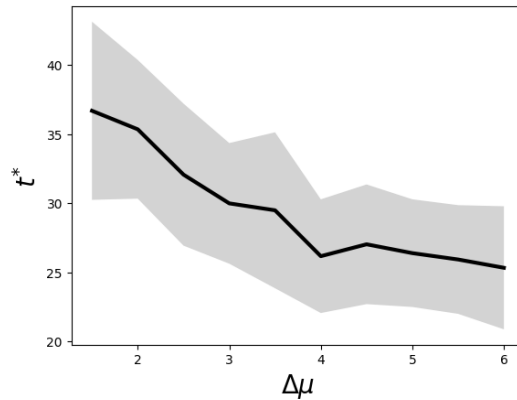


Figure 5: Effect of the distance between Gaussian means on the time it takes to converge to a single silo. Each value of $\Delta\mu$ was simulated 50 times with the line indicating the average and the shaded region indicating ± 5 SE.

In general, our results show many similarities between the behavior of systems of interacting GMMs and systems of interacting LLMs between the two experiments. However, two main differences show up between the LLM and GMM behavior. Firstly, the system of interacting GMMs shows slow oscillatory behavior while LLM shows faster oscillatory behavior. This is likely the result of the difference in the incorporation of new information between the two models as well as inherent instability in the measurement step used for the LLM model. In the system of interacting LLM agents, the interaction step consists of updating the agent’s RAG database with the information from the neighboring agent. During the measurement step, the LLM directly pulls information from this updated RAG as context to generate a response. Thus, the interaction step has an immediate effect on the agent’s response in the following time steps. On the other hand, the GMM update combines the new information from a neighboring agent with the existing RAG set and trains the GMM. Then, the new RAG set is updated with an output with a sample from the updated GMM. This process means that at each time step, each GMM agent is not changed nearly as much and the new information is not stored permanently in the RAG set. As a result, agents require more interactions over many time steps to fully switch silos in the GMM model.

Additionally, in the LLM setting, the silo of each agent is determined by their output at each time step. While this is a necessary estimate of the agent’s perspective due to the black-box nature of LLMs, it can be highly variable, especially if the agent holds a multi-modal perspective. This is compounded by the fact that the RAG database may have many sentences with conflicting perspectives. The LLMs internal knowledge may have a preference for a certain flower, while the database may contain

information that contradicts this internal preference as well as other information within the RAG. This is an example of imperfect retrieval, which has been shown to hamper the ability of LLMs in knowledge tasks [11]. As a result, this may cause additional unpredictability in LLM output, leading to the appearance of agents that switch more readily between different silos.

In section 3.3, we additionally explore the pattern where the system converges to a single silo for large t as long as k is large so agents can communicate relatively globally. Empirically, we provide extremely strong evidence in our GMM system that this pattern always holds as long as we run the simulation for a large enough number of time steps. This is an intuitive result. As one silo begins to dominate, we expect to see agents begin to choose neighbors to update with in that dominating silo, resulting in a positive feedback loop where other silos get absorbed into the silo. Further work needs to be done to prove this and further determine what values of n , k , and p this holds for.

5 Conclusion

In this paper, we propose systems of interacting GMMs as a model that can effectively replicate much of the complexity arising from system of interacting LLMs at a fraction of the computational cost, with the added benefit of mathematical tractability. Comparisons with systems of interacting LLMs from McGuinness et al. demonstrates similarities between the two approaches in the dynamics of mirroring on social alignment and the formation of silos, particular the existence of unstable silo the dependence of siloing effects on model parameters. We address potential differences in the results by providing empirical evidence for the collapse of unstable silos into a singular stable silo for a large number of time steps.

Not only do GMMs as a proxy for LLMs hold promise, their flexibility opens other avenues of research. First, while we utilize simple one dimensional GMMs with fixed means and variances, our approach can be adjusted to use multivariate Gaussians. When the means and covariances are fixed as in our example, the multivariate vectors can provide additional meaning to the possible perspectives, for example, using cosine similarity to mark various perspectives as independent of, supportive of, or contradictory to other perspectives. We can alternatively let the means and variance vary, allowing for fine grained evolution of agents in the system. Second, in our model, we use a simple method to determine silos by looking at the largest weight in the weight vector. However, this may not capture the complexities where agents may have a multi-modal distribution over the possible perspectives. As a result, more sophisticated measurement methods can be used such as the use of clustering algorithms on the entire weight vector to provide more accurate silos of the agents. If the mean and variances are allowed to vary, this could also be taken into account when determining the similarities between agents. Third, the updating mechanism can be made more elaborate: for instance, we can change the RAG set update to follow more conventional models of human memory, taking into account similarity of information to data already in memory as well as the time the information was acquired. When the GMM is updated, we can also weight the information in the RAG set by importance. Such adjustments can also be helpful in reproducing behavior of interacting LLMs for more complex queries and for richer comparisons to an array of human interactions.

Acknowledgments and Disclosure of Funding

Funding in direct support of this work:

- Air Force Office of Scientific Research (AFOSR) Complex Networks award number FA9550-25-1-0128

References

- [1] Gati V Aher, Rosa I Arriaga, and Adam Tauman Kalai. “Using large language models to simulate multiple humans and replicate human subject studies”. In: *International Conference on Machine Learning*. PMLR. 2023, pp. 337–371.
- [2] Zhenguang Garry Cai et al. “Does ChatGPT resemble humans in language use?” In: (2023).
- [3] Peng Jiang et al. “Preventing the immense increase in the life-cycle energy and carbon footprints of llm-powered intelligent chatbots”. In: *Engineering* 40 (2024), pp. 202–210.
- [4] Patrick Lewis et al. “Retrieval-augmented generation for knowledge-intensive nlp tasks”. In: *Advances in neural information processing systems* 33 (2020), pp. 9459–9474.
- [5] Xiang Li et al. “Diffusion-lm improves controllable text generation”. In: *Advances in neural information processing systems* 35 (2022), pp. 4328–4343.
- [6] Harvey McGuinness et al. “Investigating social alignment via mirroring in a system of interacting language models”. In: *arXiv preprint arXiv:2412.06834* (2024).
- [7] Zhijie Nie et al. “When Text Embedding Meets Large Language Model: A Comprehensive Survey”. In: *arXiv preprint arXiv:2412.09165* (2024).
- [8] Zach Nussbaum et al. “Nomic embed: Training a reproducible long context text embedder”. In: *arXiv preprint arXiv:2402.01613* (2024).
- [9] Hugo Touvron et al. “Llama 2: Open foundation and fine-tuned chat models”. In: *arXiv preprint arXiv:2307.09288* (2023).
- [10] Ashish Vaswani et al. “Attention is all you need”. In: *Advances in neural information processing systems* 30 (2017).
- [11] Fei Wang et al. “Astute rag: Overcoming imperfect retrieval augmentation and knowledge conflicts for large language models”. In: *arXiv preprint arXiv:2410.07176* (2024).
- [12] Xiao Wang et al. “State space model for new-generation network alternative to transformers: A survey”. In: *arXiv preprint arXiv:2404.09516* (2024).